JACS
JOURNAL OF THE AMERICAN CHEMICAL SOCIETY
pubs.acs.org/JACS

Article

CXC Chemokine Ligand 12 Facilitates Gi Protein Binding to CXC Chemokine Receptor 4 by Stabilizing Packing of the Proline−Isoleucine−Phenylalanine Motif: Insights from Automated Path Searching

Xinyu Li,[§] Yezhou Liu,[§] Jinchu Liu, Wenzhuo Ma, Rujuan Ti, Arieh Warshel,* Richard D. Ye,* and Lizhe Zhu*

Cite This: J. Am. Chem. Soc. 2025, 147, 10129−10138

Read Online

ACCESS | Metrics & More | Article Recommendations | Supporting Information

ABSTRACT: The activation of G protein-coupled receptors (GPCRs) is a complex multibody multievent process involving agonist binding, receptor activation, G protein coupling, and subsequent G protein activation. The order and energetics of these events, though crucial for the rational design of selective GPCR drugs, are challenging to characterize and remain largely underexplored. Here, we employed molecular dynamics simulations and our recently developed traveling salesman-based automated path searching (TAPS) algorithm to efficiently locate the minimum free-energy paths for the coupling events of the CXC chemokine receptor 4 (CXCR4) with its endogenous ligand CXC chemokine ligand 12 (CXCL12) and Gi protein. We show that, after overcoming three low energy barriers (3.24−6.89 kcal/mol), Gi alone can precouple with CXCR4 even without CXCL12, consistent with previous reports on the existence of the apo CXCR4-Gi complex and our NanoBiT experiments. The highest barrier of 6.89 kcal/mol in this process corresponds to the packing of the proline−isoleucine−phenylalanine (PIF) motif of CXCR4. Interestingly, without Gi, CXCL12 alone cannot activate CXCR4 (high barrier of 18.89 kcal/mol). Instead, it can enhance Gi coupling by circumventing the energy barrier of PIF packing. Shedding new light on the activation mechanism of CXCR4, these results present TAPS as a promising tool for uncovering complete activation pathways of GPCRs and the corresponding agonist design.

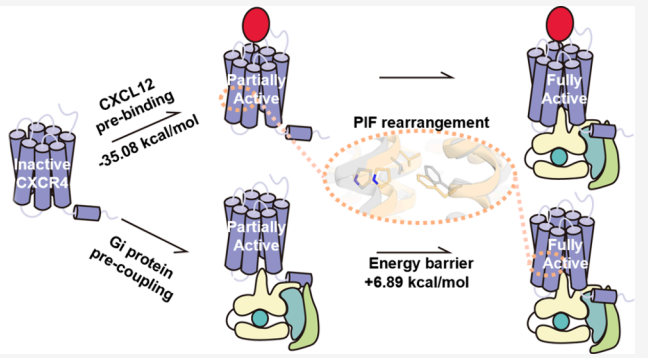

1. INTRODUCTION

G protein-coupled receptors (GPCRs), also known as seven-transmembrane domain receptors, can detect molecules outside the cell and transmit the extracellular signal into the cell through coupling with G proteins.[1] The human GPCR family is divided into four major classes based on their amino acid sequences and structural features: class A (rhodopsin family), class B (secretin and adhesion family), class C (glutamate family), and class F (Frizzled family) subfamilies. Over 800 genes in the human genome are found expressing GPCRs, and over 500 GPCR drugs target class A GPCRs. Biochemical and biophysical data have demonstrated that GPCRs are inherently flexible and dynamic proteins. Their activation is a complex multibody and multistep process that involves a series of intermediate conformational states,[2−5] including agonist binding, receptor activation, G protein coupling, and subsequent G protein activation.[6−8] A general idea (Figure 1A) is the ligand prebinding model[9] that the agonist initially binds to a GPCR, inducing the GPCR to shift its conformation toward the activated state where the cavity on the cytoplasmic side was opened for G protein binding. Upon the G protein couples to the receptor, the nucleotide-binding pocket lying between the Ras-homology domain (RHD) and the α-helical (AH) domain opens to release the GDP and receives GTP. However, experimental[10−12] and computational results[13] have revealed that most potent agonists alone cannot stabilize GPCRs in their fully active conformation. Moreover, existing structures of the GPCR-G protein complexes,[14−17] as well as previous computational[17,18] and experimental studies,[19−21] have pointed out that G proteins can couple with the GPCRs even in the absence of agonists. Based on these findings, a second model, G protein precoupling model[18,22] (Figure 1B), has been proposed, which suggests that G protein

Received: October 13, 2024
Revised: February 15, 2025
Accepted: February 19, 2025
Published: March 17, 2025

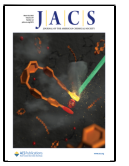

https://doi.org/10.1021/jacs.4c14293
J. Am. Chem. Soc. 2025, 147, 10129−10138

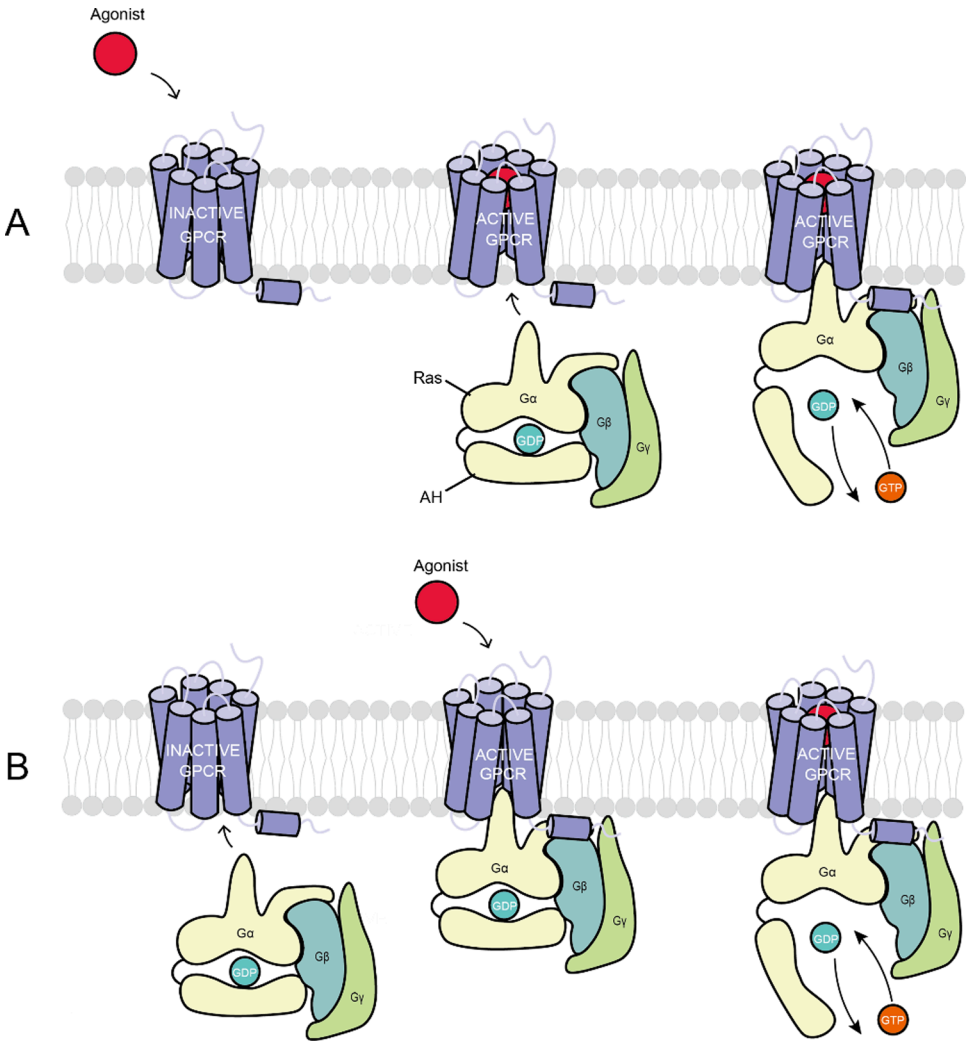

Figure 1. Two modes of the activation process of class A GPCRs: (A) ligand prebinding model; (B) G protein precoupling model.

may first bind to GPCR, leading to an intermediate state of the receptor-G protein complex, to which the agonist may bind and then propagate to full activation. In other words, the G protein can couple to the GPCR without the help of an agonist. To the best of our knowledge, no systematic comparison between these two models for GPCR activation has been conducted to date.

Structural biology techniques typically can provide high-resolution atomistic structures for only an inactive state (bound to antagonists) or a fully active state (bound to agonists and G proteins). However, it is difficult for them to capture intermediate states, particularly the critical, short-lived transition state, which represents the highest energy point along the reaction coordinate and acts as a critical "bottleneck" for the transition between two stable intermediate states. Characterizing the transition state and its associated free-energy barriers is essential for advancing our understanding of GPCR activation mechanisms.[6−8,23] For example, the energy barriers along the activation pathways of S1P receptors, which are activated by different agonists, provide insights into the agonist selectivity for specific S1P receptor subtypes.[23]

MD-based path searching methods can locate the minimum free-energy path (MFEP) of the transition process between the two states of interest, which is practical for identifying transition states, stable intermediate states, and their corresponding energy barriers along the transition process.[24−29] Typically, path searching methods begin with an initial guess path for the transition process, defined in a specific coordinate space composed of a few preselected collective variables (CVs). Sampling is then conducted at each node along the path to explore low-energy conformations, followed by path reparameterization to reconstruct the path using these sampled low-energy states. Through iterative refinements, the path converges to the MFEP that is closest to the initial guess path. However, the efficiency of most path-based methods[25−28] is limited by two key factors: (1) the preselection of CVs with well-defined physical meaning requires sufficient prior knowledge of the system and incorrectly defined CVs can result in tedious iterative input validation;[30] (2) local sampling at each node leads to slow convergence of the path toward the MFEP.

To tackle these issues, our group developed the traveling salesman-based automated path searching (TAPS) algorithm,[31] an all-atom MD simulation-based automated path searching approach. In TAPS, instead of choosing static CVs, path collective variables (PCVs)[32] are employed as the temporary coordinate system for each iteration. PCVs require only a distance metric as input such as the root-mean-square deviation (RMSD) between any pair of conformations, thereby minimizing the need for prior knowledge about the system. Moreover, nonlocal perpendicular sampling at each node

https://doi.org/10.1021/jacs.4c14293
J. Am. Chem. Soc. 2025, 147, 10129−10138

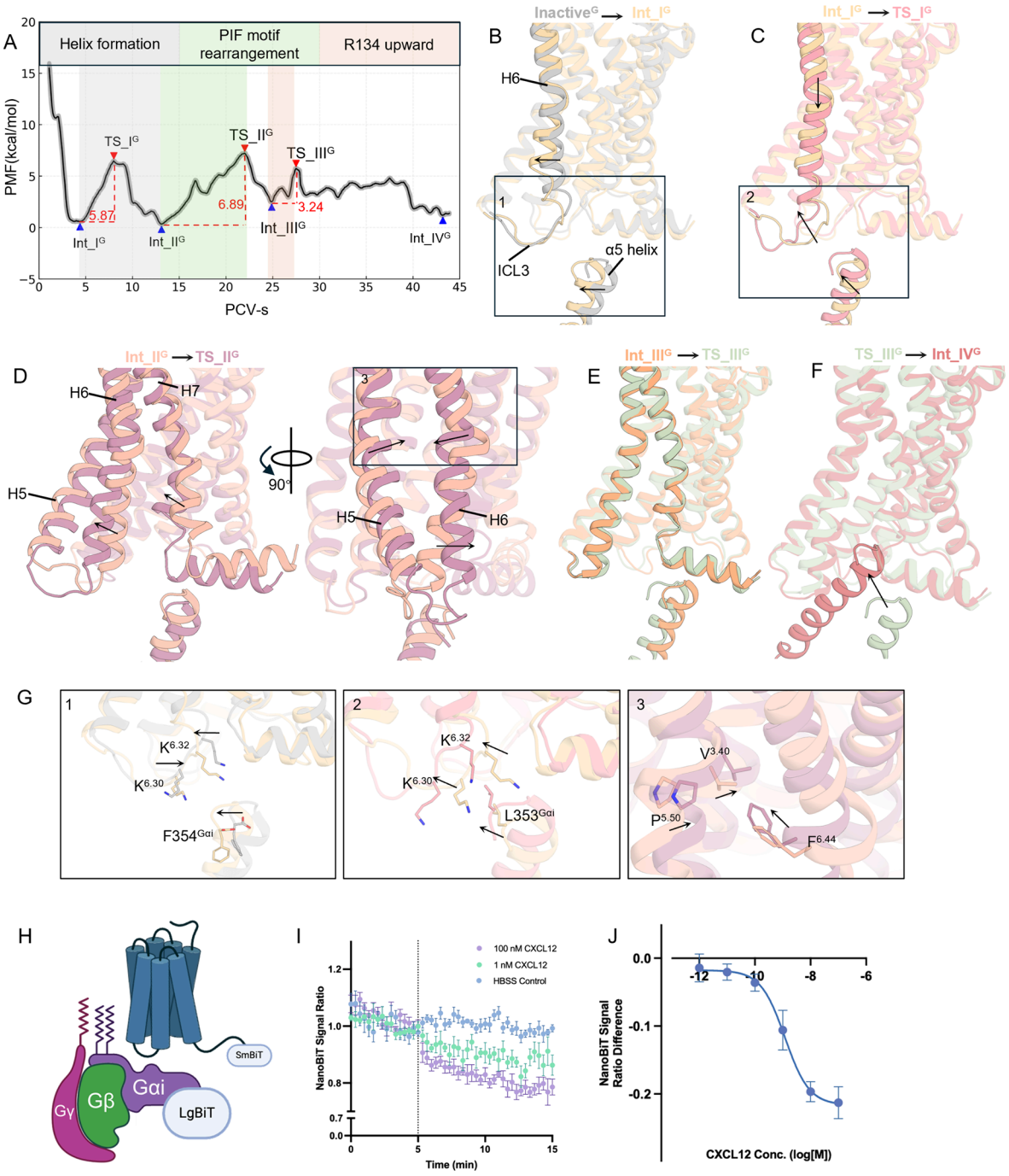

Figure 2. Analysis of Path^G. (A) Free-energy landscape of Path^G along the PCVs with the transparent bands denoting the errors. (B) Conformational change from Inactive^G to Int_I^G. (C) Conformational change from Int_I^G to TS_I^G. (D) Two different views of conformational change from Int_II^G to TS_II^G. (E) Conformational change from Int_III^G to TS_III^G. (F) Conformational change from TS_III^G to Int_IV^G. From panels (B−F), we show only the α5 helix of Gi for better visualization. (G) Conformation changes in detail. G-1 to G-3 correspond to the rectangular region in panels (B−D), respectively. (H) Schematic illustration of a NanoBiT-based Gi activation assay. NanoLuc was split into an SmBiT subunit and an LgBiT subunit. The SmBiT subunit was fused to the C-terminus of CXCR4, and the LgBiT subunit was attached to the Gαi protein. (I) The NanoBiT-based Gαi activation assay, involving coexpression of CXCR4-SmBiT and LgBiT-Gαi in HEK293 cells, unravels Gαi dynamics upon CXCL12 stimulation. Baseline NanoBiT signals were recorded for 5 min, followed by the addition of CXCL12 at varying concentrations. Readouts were collected for an additional 10 min. NanoBiT signal ratio data were normalized as (NanoBiT signal/average of baseline NanoBiT signal) from three independent experiments, each performed in duplicate, and are presented as the mean ± SEM. (J) Dose−response curve of CXCL12-induced Gαi dynamics from panel (I). The change in NanoBiT signal ratio was calculated as (average NanoBiT signal ratio after CXCL12 stimulation − average baseline NanoBiT signal ratio). Data were collected from three independent experiments, each in duplicate, and are presented as the mean ± SEM.

accelerates the search for low-free-energy conformations. TAPS has been successfully applied to the biomolecule systems of tens to hundreds of residues[33−38] and particularly in the fine design of selective agonists for the sphingosine 1-phosphate receptor (S1PR) family (class A GPCRs),[23] where we accurately evaluated the selectivity of agonist targeting

https://doi.org/10.1021/jacs.4c14293
J. Am. Chem. Soc. 2025, 147, 10129−10138

distinct S1PR subtypes by selecting all the heavy atoms within the transmembrane helices and agonists to define PCV. This unbiased atom selection makes TAPS particularly suitable for studying class A GPCRs due to their conserved structural topology.[39]

CXC chemokine receptor 4 (CXCR4) belongs to the class A GPCRs, it is widely expressed in human tissue and plays an important role in diverse biological processes, such as angiogenesis,[40] embryonic development,[41] homing regulation of hematopoietic stem cells,[42,43] metastasis,[44−47] and immune cell chemotaxis toward its endogenous ligand CXC chemokine ligand 12 (CXCL12).[48] In addition, CXCR4 also functions as a coreceptor for HIV-1 entry into CD4+ cells.[49] Targeting CXCR4 has been proposed as a promising strategy in terms of CXCR4/CXCL12 signal related cancers,[50] HIV,[49] autoimmunity, as well as inflammation.[51,52] Currently, three CXCR4 antagonists (Plerixafor, Mavorixafor, and Motixafortide) have been approved by the FDA, and three CXCR4 agonists (ATI-2341,[53] NUCC-390,[54] CTCE-0214[55]) are under development. The crystal structures of CXCR4 bound to various antagonists have been resolved several years ago.[56,57]

Recently, we reported the Cryo-EM structure of the active state of CXCR4 bound to CXCL12.[58] Compared to the inactive state, the fully active conformation of CXCR4 shows several common activation features that characteristic of most class A GPCRs[59] involving the significant tilt of the helix 6 (H6), upward movement of the R134$^{3.50}$(GPCRdb numbering[60]) in the DRY motif, the inward rotation of the Y302$^{7.53}$ in the NPxxY motif, and packing of V124$^{3.40}$, P211$^{5.50}$, and F248$^{6.44}$ residues (PIF motif). Additionally, we observed an intriguing structural difference in the reported CXCR4 structures (Table. S1). When the CXCR4 structure is resolved in complex with the Gi, residues Q233^{ICL3} to A237$^{6.33}$ consistently adopt a helical conformation. But in the absence of the Gi, these residues display variability, with some adopting a helical structure, others forming a loop, or even being unresolved in the structures. However, the precise mechanisms underlying the conformational changes induced by CXCL12 binding or Gi coupling remain poorly understood.

In this work, we employed MD simulations combined with TAPS algorithm to explore the activation mechanism of CXCR4 in the G protein precoupling model and the ligand prebinding model. To explore the activation processes of the CXCR4 in the G protein precoupling model, we designed Path^{G} (Figure S2A), where Gi couples to the CXCR4^{apo} in the absence of CXCL12. To explore the activation process of CXCR4 in the general ligand prebinding model, we designed Path^{L} (Figure S2B), where CXCL12 shifts the CXCR4^{apo} to its fully active state without Gi, and Path^{LG} (Figure S2C), where Gi couple to CXCR4 with exits of CXCL12. For each of these paths, the initial trajectory was generated using targeted molecular dynamics (tMD)[61] and subsequently optimized using the TAPS method to locate the MFEP. Finally, umbrella sampling[62] was employed to obtain the free-energy landscape along the MFEP, providing further insights into the energetics of CXCR4 activation. The free-energy landscape of Path^{G} reveals that the Gi can precouple with CXCR4, forming a stable CXCR4-Gi complex that shifts CXCR4 into its active conformation, but must overcome a barrier of ∼6.89 kcal/mol for rearranging the PIF motif. NanoBiT assays and the recently reported apo CXCR4-Gi complex (PDB code: 8U4N) support the occurrence of precoupling events. By contrast, the free-energy landscapes of Path^{L} and Path^{LG} indicate that CXCL12 alone is insufficient to activate CXCR4. Instead, CXCL12 forms a stable complex with CXCR4, where the packing of the PIF motif is stabilized in a pure energy-releasing process. Consequently, energy consumption by subsequent Gi coupling for rearranging the PIF is no longer necessary. Overall, our study provides an atomistic description of CXCR4 activation in both the ligand prebinding and the G protein precoupling models and presents a valuable framework for investigating the activation mechanisms of other class A GPCRs.

2. RESULTS

2.1. Gi Can Precouple to CXCR4 without CXCL12. To examine whether Gi alone can couple to CXCR4 and shift it to the fully active state before CXCL12 binds to the receptor, we evaluated the energetics of Path^{G}, a transition process in which Gi couples to the inactive CXCR4^{apo} to form the active CXCR4-Gi complex. To characterize the active state of CXCR4, we selected three conserved conformational changes typically observed in most class A GPCRs: (1) the tilt angle of H6, (2) the upward movement of R134$^{3.50}$, and (3) the inward rotation angle of Y302$^{7.53}$ (Figure S3). Along Path^{G}, three energy barriers (5.87, 6.89, and 3.24 kcal/mol, Figure 2A) were identified, none of which are sufficiently high to prevent the transition. In other words, Gi can couple to inactive CXCR4^{apo} to form the active CXCR4-Gi complex, even in the absence of CXCL12.

To elucidate the mechanism of this transition, we analyzed the structural changes for each intermediate state in detail. First, the free-energy curve decreases until Int_I^{G}, where the α5 helix of the Gαi protein moves closer to ICL3 and H6 of CXCR4 (Figure 2B). This movement is driven by electrostatic attraction between the positively charged residues K234$^{6.30}$ and K236$^{6.32}$ and the negatively charged residue F354$^{Gi\alpha}$ (Figure 2G-1, Figure S4A). Consequently, this induces a partial tilt of H6 (Figure S3A, Table S7). Following this, a moderate energy barrier (5.87 kcal/mol) exists between Int_I^{G} and TS_I^{G}. At this stage, the structural part of H6 shows a downward movement (Figure 2C). However, hydrophobic residue L353 in Gi approaches hydrophilic residues K234$^{6.30}$ and K236$^{6.32}$ (Figure 2G-2), which push the upward movement of the intracellular loop 3 (ICL3) and unstructured part in H6. As a result, these face-to-face movements compact H6 on the cytoplasmic side, leading to the formation of a helical structure from R235$^{6.31}$ to A237$^{6.33}$ in Int_II^{G} (Figure S4D). Next, another moderate energy barrier (6.89 kcal/mol) is observed from Int_II^{G} to TS_II^{G}. During this phase, a synergetic rearrangement appearing between P211$^{5.50}$, V124$^{3.40}$, and F248$^{6.44}$ (PIF motif) makes the F248$^{6.44}$ close to P211$^{5.50}$ and V124$^{3.40}$ (Figure 2G-3, Figure S4B), which initiate the outward swing of the cytoplasmic part of H6 (Figure 2D). Then, the Y302$^{7.53}$ could move deeper into the inner side of CXCR4. Finally, there is a small energy barrier (3.24 kcal/mol) between Int_III^{G} and TS_III^{G}, corresponding to the upward movement of R134$^{3.50}$. The activation features in TS_III^{G} (Figure 2E, Figure S4C) indicate the fully activated state of CXCR4, wherein the Gi can fully couple to CXCR4 (Figure 2F).

To validate our computational finding that Gi can couple to CXCR4 in the absence of CXCL12, we conducted a NanoBiT-based Gαi activation assay. In this assay, a SmBiT subunit of NanoLuc was fused to the C-terminus of CXCR4, and an LgBiT subunit was attached to the Gαi (Figure 2H). This setup allowed us to monitor the relative distance between the

https://doi.org/10.1021/jacs.4c14293
J. Am. Chem. Soc. 2025, 147, 10129−10138

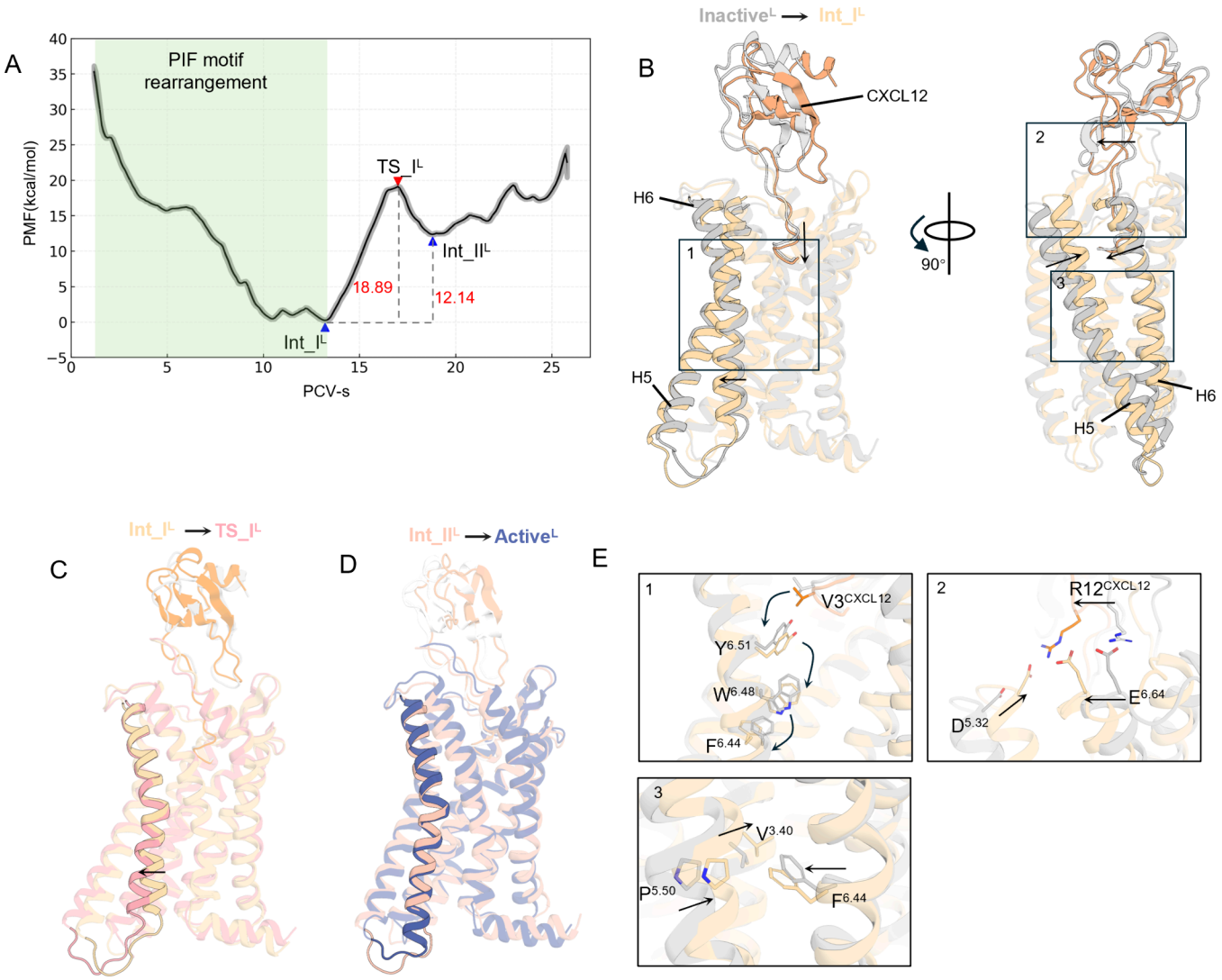

Figure 3. Analysis of Path^{L}. (A) Free-energy landscape of the Path^{L} along the PCVs with the transparent bands denoting the errors. (B) Two different views of conformational change from Inactive^{L} to Int_I^{L}. Inactive^{L} is the last frame generated from the initial path of the Path^{L}. (C) Conformational change from Int_I^{L} to TS_I^{L}. (D) Conformational change from Int_II^{L} to Active^{L}. (E) Conformation changes in detail. E1−E3 correspond to the rectangular region in panels (B−D), respectively.

C-terminus of CXCR4 and Gαi through bioluminescence signal amplitudes, with stronger signals indicating closer proximity between the two proteins. The NanoBiT-based Gαi activation assay enabled us to track the changes in a distance between CXCR4 and Gαi during receptor activation. Initially, a strong bioluminescence signal indicated that Gαi is close enough to CXCR4. Upon ligand addition, the distance between CXCR4 and Gαi increases rapidly (Figure 2I), demonstrating concentration-dependent dissociation of Gαi from CXCR4 that increased with higher CXCL12 concentrations (Figure 2J). Furthermore, the recently resolved structure of the apo CXCR4-Gi complex (PDB code: 8U4N) also indicates that the Gi can couple to CXCR4 in the absence of CXCL12. Collectively, these experimental results support our computational findings, confirming that Gi can couple with CXCR4 and without the presence of the CXCL12.

2.2. CXCL12 Stabilizes CXCR4 in an Intermediate State. Generally, it has been assumed that the agonists bind to GPCRs and shift their equilibrium to an active state, which shows the remarkable tilt of H6 and the expansion of intracellular region to facilitate recruitment of the G protein. To examine whether CXCL12 alone could shift CXCR4 to its fully active state in the absence of Gi, we evaluated the energetics of Path^{L} (Figure 3A). Similarly, we selected three features, the same as Path^{G} to define the active state of the CXCR4. Along Path^{L}, a remarkable energy barrier (18.89 kcal/mol) is observed between Int_I^{L} and TS_I^{L}, corresponding to the significant tilt of helix 6 (Figure 3C), which is an activation feature of the CXCR4. However, such a high barrier indicates that the activation of CXCR4 by CXCL12 alone is difficult. Additionally, the high energy difference (12.14 kcal/mol) between Int_I^{L} and Int_II^{L} indicates the instability of Int_II^{L}, which is consistent with previously experimental[10−12] and computational results[13] that the agonist alone cannot stabilize GPCR in its fully active conformation. Consequently, without Gi, CXCL12 alone cannot fully activate CXCR4; instead, it binds to CXCR4 and then stabilizes in the Int_I^{L} state, awaiting coupling of Gi.

To elucidate the conformational changes of CXCR4 induced by CXCL12, we analyzed the key intermediate states in detail. We observed that the energy curve decreases to the Int_I^{L} as CXCL12 penetrates deeper into the binding pocket.

https://doi.org/10.1021/jacs.4c14293
J. Am. Chem. Soc. 2025, 147, 10129−10138

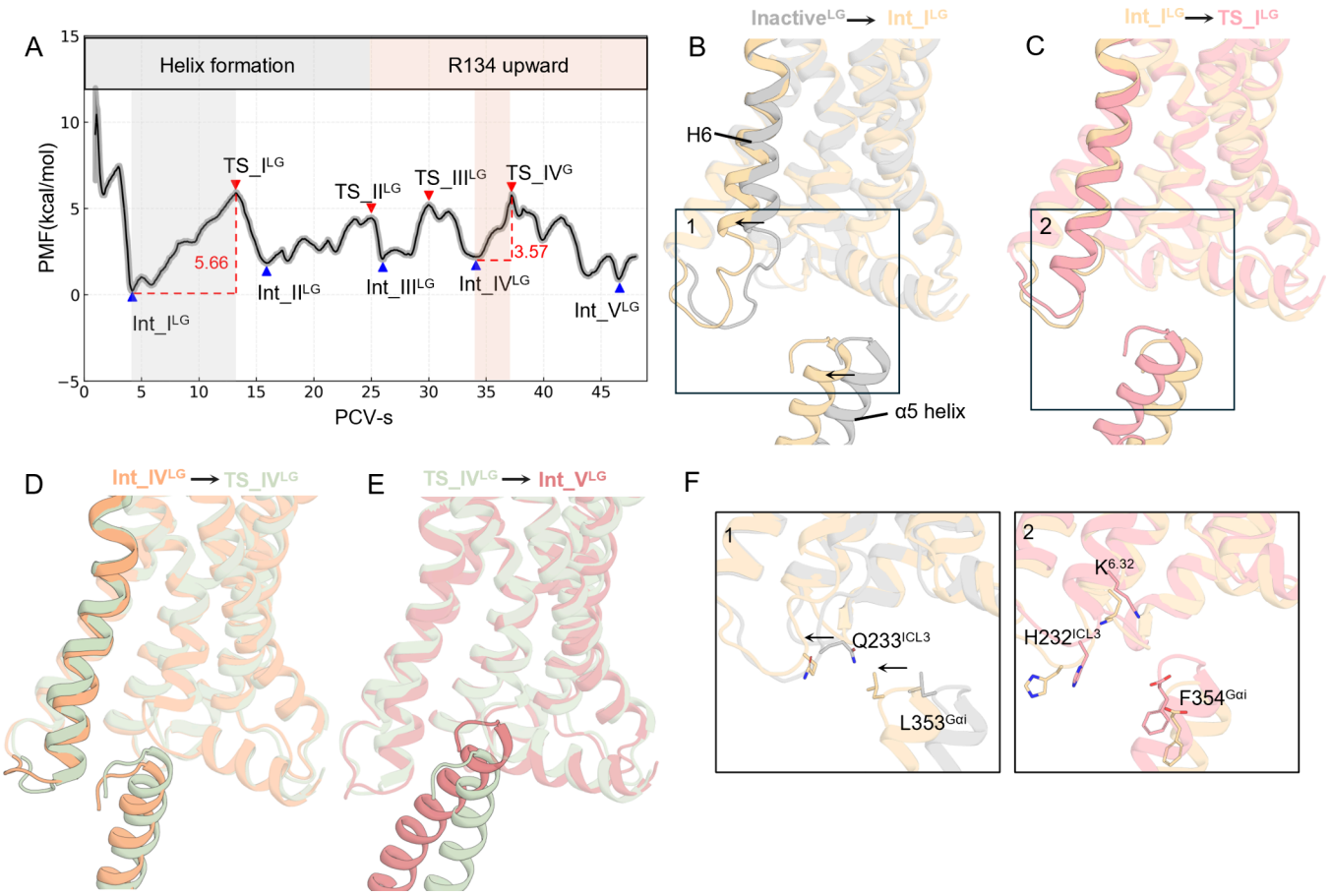

Figure 4. Analysis of Path^{LG}. (A) Free-energy landscape of Path^{LG} along the PCVs with the transparent bands denoting the errors. (B) Conformational changes from Inactive^{LG} to Int_I^{LG}. (C) Conformational change from Int_I^{LG} to TS_I^{LG}. (D) Conformational changes from Int_IV^{LG} to TS_IV^{LG}. (E) Conformational change from TS_IV^{LG} to Int_V^{LG}. (F) Conformation changes are shown in detail. F1 and F2 correspond to the rectangular region in panels (B) and (C), respectively. We only show the α5 helix of Gi for better visualization.

Specifically, V3 of CXCL12 induces a downward movement of Y255$^{6.51}$, which in turn pushes W252$^{6.48}$ downward, subsequently triggering the outward movement of F248$^{6.44}$ (Figure 3E-1). Additionally, R12^{CXCL12} interacts with D193$^{5.32}$ and E268$^{6.64}$ (Figure 3E-2), inducing the packing of helices H5 and H6 (Figure 3B, Figure S5A). This interaction brings P211$^{5.50}$ closer to F248$^{6.44}$ (Figure 3E-3, Figure S5B). These conformational changes lead to the synergistic rearrangement of the PIF motif (P211$^{5.50}$, V124$^{3.40}$, and F248$^{6.44}$), initiating a partial tilt of H6 (Figure S3B, Table S7). Interestingly, this free-energy-decreasing rearrangement of the PIF motif contrasts with the second energy barrier in Path^{G}. The previous experiment[63] has shown that mutation of R12E in CXCL12 significantly decreases downstream signaling, also highlighting the importance of R12^{CXCL12}. In addition, we found that although the residues R235$^{6.31}$ to A237$^{6.33}$ in Active^{L} show a helical structure (Figure 4D, Figure S5D), they exhibit nonhelical structure in the transition from Inactive^{L} to Int_II^{L} (Figure S5D). However, in Path^{G}, these five residues form a stable helical structure in Int_III^{G} with the assistance of the Gi, suggesting that the Gi may contribute to the formation of the helical structure on the cytoplasmic side of H6.

2.3. CXCL12 Stabilizes Packing of the PIF Motif to Facilitate Gi Coupling. Path^{L} verified that CXCL12 can partially activate CXCR4 by inducing the tilt of H6, stabilizing CXCR4 in Int_I^{L} rather than shifting it completely to its fully active state. This observation led us to hypothesize that this partial tilting of H6 could facilitate Gi coupling more effectively. To test this hypothesis, we evaluated the energetics of Path^{LG}. Compared to Path^{G}, we observed only two moderate energy barriers (5.66 and 3.57 kcal/mol) in Path^{LG} (Figure 4A), indicating that the partial activation of CXCR4 induced by CXCL12 decreases the energy barrier for subsequent Gi coupling. Similarly, compared to Path^{L}, Path^{LG} significantly decreases the energy barrier for CXCR4 activation, indicating that Gi is necessary for the full activation of CXCR4.

To clarify the process that the Gi couples to the CXCR4-CXCL12 complex, we analyzed the key conformational states in detail. Initially, the free-energy curve decreases until it reaches the Int_I^{LG} state, where the hydrophobic residue L353$^{G\alpha i}$ in the α5 helix of the Gαi moves closer to the ICL3 and H6 of CXCR4. This interaction causes L353$^{G\alpha i}$ to push the hydrophilic residue Q233^{ICL3} (Figure 4F-1), inducing a tilt of H6 (Figure 4B). Subsequently, there is an energy barrier (5.66 kcal/mol) between Int_I^{LG} and TS_I^{LG}, corresponding to the formation of a helical structure in residues Q233^{ICL3} to A237$^{6.33}$ (Figure 4C, Figure S6B). This conformational change is driven by the electrostatic attraction between the positively charged residues H232^{ICL3} and K236$^{6.32}$ and the negatively charged residue F354$^{G\alpha i}$ (Figure 4F-2, Figure S6A). From Int_II^{LG} to Int_IV^{LG}, there is no significant energy barrier during these transitions, suggesting that the complex may fluctuate between these states (Figures S6B and S7). In the

https://doi.org/10.1021/jacs.4c14293
J. Am. Chem. Soc. 2025, 147, 10129−10138

TS_IV^{LG} state, the upward movement of R134$^{3.50}$ (Figure S6B) signifies that CXCR4 has reached its fully activated conformation. This structural change allows Gi to fully couple to CXCR4 in the subsequent Int_V^{LG} state (Figure 4E).

3. DISCUSSION

Most previous studies on GPCR activation[5,64,65] have focused only on receptor activation by the agonist, without considering the effects of the G protein. Here, we investigate the activation of not only the receptor but also the subsequent G protein coupling, using the CXCL12-CXCR4-Gi complex as a model system. The highest energy barriers observed in Path^{G} (6.89 kcal/mol) and Path^{LG} (5.66 kcal/mol) are relatively similar, suggesting that CXCR4 activation may involve both paths. The activation paths that CXCR4 follows depend on the sequence of CXCL12 binding and Gi coupling. Path^{G} aligns with the Gi precoupling model, in which Gi alone can precouple with CXCR4, shifting CXCR4 to its fully active state. Conversely, Path^{L} and Path^{LG} follow the ligand prebinding model with a slight variation that CXCL12 binding alone does not fully stabilize CXCR4 in its active conformation, and Gi coupling is still required for complete activation. The role of CXCL12 is to bind to CXCR4 to form a stable CXCL12-CXCR4 complex (Int_I^{L}). This complex circumvents the secondary energy barrier observed in Path^{G} by stabilizing the packing of the PIF motif, thereby facilitating subsequent Gi coupling. Moreover, Gi plays a critical role in CXCR4 activation by pushing the H6 helix outward, shifting R134$^{3.50}$ upward, and stabilizing the helical structure within the region of Q233^{ICL3}–A237$^{6.33}$. These structural changes collectively facilitate receptor activation. In addition, as shown in Table S4, rather than selecting specific atoms to define the PCVs, we adopt an unbiased selection of atom set, which is generalizable to other chemokine receptors and G proteins due to their similar structural topologies[66,67] and potentially to the study of the activation of all class A GPCRs. These results present TAPS as a promising approach in boosting a comprehensive understanding of the activation mechanisms of class A GPCRs.

Despite the aforementioned merits, our results remain limited and warrant further investigation. First, the NanoBiT assay employed in this study does not directly validate the free-energy landscapes associated with the activation process of CXCR4. For example, it does not provide direct insights into the free-energy changes related to packing of the PIF motif. Future studies via techniques such as nuclear magnetic resonance (NMR)[68−70] could be necessary to examine the subtle conformational changes and the corresponding energetics found in the present work. Second, we note that the full activation of GPCRs involves not only the activation of the GPCR but also the activation of G protein. In addition to the role of CXCL12 binding in facilitating Gi coupling, our finding that Gi can precouple with CXCR4 even in the absence of CXCL12 point to the potential role of CXCL12 binding to Gi activation, which has not been covered in the present work but worth further studies. Previous computational analyses[71] have demonstrated that the β2-adrenergic receptor (β2AR) exhibits distinct effects on the opening of the AH and RHD depending on whether it is bound to an agonist, a reverse agonist, or is in an apo state. However, how different ligands induce these effects remain unclear. In the future, we shall further investigate the activation process of Gi to elucidate this potential effect of CXCL12 binding. Third, biased signaling, where distinct ligands binding to a GPCR preferentially activate specific signaling pathways, such as the G protein or β-arrestin pathways, presents significant potential for the development of safer and more effective drugs. In the context of CXCR4, both the K1R mutant[72] of its endogenous ligand CXCL12 and the synthetic agonist ATI-2341[73] exhibit bias toward G protein-coupled signaling. Despite these findings, the structural basis of this biased signaling is poorly understood. Our future research will focus on uncovering the molecular mechanisms driving these conformational changes, thereby providing crucial insights into biased signaling and its potential applications in drug development.

4. CONCLUSIONS

In this study, we applied all-atom molecular dynamics simulations and our recently matured automated path searching method (TAPS) to reveal the detailed energetics and order of events for the activation of CXCR4 by its natural agonist CXCL12. Consistent with previous findings and our NanoBiT experiments, our calculations show that the Gi protein can precouple with CXCR4 in the absence of CXCL12. To achieve such precoupling, Gi only needs to overcome three low energy barriers (3.24−6.89 kcal/mol), where the highest barrier corresponds to the packing of the PIF motif. In addition, the binding of CXCL12 alone cannot activate CXCR4 due to a substantial energy barrier (18.89 kcal/mol); it facilitates Gi coupling through bypassing the barrier for PIF packing. These detailed mechanistic insights demonstrate not only the power of TAPS in dissecting the multievent process of GPCR activation but also its potential for guiding the rational design of GPCR agonists.

■ ASSOCIATED CONTENT

Supporting Information

The Supporting Information is available free of charge at https://pubs.acs.org/doi/10.1021/jacs.4c14293.

Simulation methods and supplementary results(PDF)

■ AUTHOR INFORMATION

Corresponding Authors

Arieh Warshel − *Department of Chemistry, University of Southern California, Los Angeles, California 90089, United States;* orcid.org/0000-0001-7971-5401; Email: warshel@usc.edu

Richard D. Ye − *Kobilka Institute of Innovative Drug Discovery, School of Medicine, The Chinese University of Hong Kong, Shenzhen, Guangdong 518172, China; The Chinese University of Hong Kong, Shenzhen Futian Biomedical Innovation R&D Center, Shenzhen, Guangdong 518048, China;* orcid.org/0000-0002-2164-5620; Email: richardye@cuhk.edu.cn

Lizhe Zhu − *School of Medicine and Warshel Institute for Computational Biology, The Chinese University of Hong Kong, Shenzhen, Guangdong 518172, China;* orcid.org/0000-0001-8252-7807; Email: zhulizhe@cuhk.edu.cn

Authors

Xinyu Li − *School of Medicine and Warshel Institute for Computational Biology, The Chinese University of Hong Kong, Shenzhen, Guangdong 518172, China*

Yezhou Liu − *Kobilka Institute of Innovative Drug Discovery, School of Medicine, The Chinese University of Hong Kong,*

Shenzhen, Guangdong 518172, China; orcid.org/0000-0001-7575-8260

Jinchu Liu − *School of Medicine and Warshel Institute for Computational Biology, The Chinese University of Hong Kong, Shenzhen, Guangdong 518172, China*

Wenzhuo Ma − *School of Medicine and Warshel Institute for Computational Biology, The Chinese University of Hong Kong, Shenzhen, Guangdong 518172, China*

Rujuan Ti − *School of Medicine and Warshel Institute for Computational Biology, The Chinese University of Hong Kong, Shenzhen, Guangdong 518172, China;* orcid.org/0000-0002-5169-8491

Complete contact information is available at: https://pubs.acs.org/10.1021/jacs.4c14293

Author Contributions

[§]X.L. and Y.L. contributed equally to this work

Notes

The authors declare no competing financial interest.

■ ACKNOWLEDGMENTS

This work was supported by National Natural Science Foundation of China Projects 32471296 (L.Z.) and 32070950 (R.D.Y.) and Science, Technology, and Innovation Commission of Shenzhen Municipality Projects JCYJ-20200109150003938 (L.Z.), RCYX20200714114645019 (L.Z.), and GXWD20201231155722002-20200831175432002 (L.Z. and R.D.Y.). L.Z. was also supported in part by a Presidential Fellowship. This work is supported by the Warshel Institute for Computational Biology funding from Shenzhen City and Longgang District (LGKCSDPT2024001). This work is also supported by National Key R&D Program of China grant 2019YFA0906003 (R.D.Y.), Yunnan Key Research and Development Program grant 202402AA310032 (R.D.Y.), Shenzhen Medical Research Fund SMRF-D2403009 (R.D.Y.), the Kobilka Institute of Innovative Drug Discovery at The Chinese University of Hong Kong, Shenzhen. (R.D.Y.), the Ganghong Young Scholar Development Fund (R.D.Y.), and Shenzhen-Hong Kong Cooperation Zone for Technology and Innovation grant HZQB-KCZYB-2020056(R.D.Y.). X.L. was supported by the Ganghong Young Scholar Development Fund at The Chinese University of Hong Kong, Shenzhen.

■ REFERENCES

(1) Trzaskowski, B.; Latek, D.; Yuan, S.; Ghoshdastider, U.; Debinski, A.; Filipek, S. Action of molecular switches in GPCRs–theoretical and experimental studies. *Curr. Med. Chem.* **2012**, *19* (8), 1090−1109.

(2) Kobilka, B. K.; Deupi, X. Conformational complexity of G-protein-coupled receptors. *Trends Pharmacol. Sci.* **2007**, *28* (8), 397−406.

(3) Ye, L.; Van Eps, N.; Zimmer, M.; Ernst, O. P.; Scott Prosser, R. Activation of the A2A adenosine G-protein-coupled receptor by conformational selection. *Nature* **2016**, *533* (7602), 265−268.

(4) Wang, X.; Neale, C.; Kim, S. K.; Goddard, W. A.; Ye, L. Intermediate-state-trapped mutants pinpoint G protein-coupled receptor conformational allostery. *Nat. Commun.* **2023**, *14* (1), 1325.

(5) Lu, S.; He, X.; Yang, Z.; Chai, Z.; Zhou, S.; Wang, J.; Rehman, A. U.; Ni, D.; Pu, J.; Sun, J.; et al. Activation pathway of a G protein-coupled receptor uncovers conformational intermediates as targets for allosteric drug design. *Nat. Commun.* **2021**, *12* (1), 4721.

(6) Alhadeff, R.; Vorobyov, I.; Yoon, H. W.; Warshel, A. Exploring the free-energy landscape of GPCR activation. *Proc. Natl. Acad. Sci. U. S. A.* **2018**, *115* (41), 10327−10332.

(7) Zhu, X.; Luo, M.; An, K.; Shi, D.; Hou, T.; Warshel, A.; Bai, C. Exploring the activation mechanism of metabotropic glutamate receptor 2. *Proc. Natl. Acad. Sci. U. S. A.* **2024**, *121* (21), No. e2401079121.

(8) Bai, C.; Wang, J.; Mondal, D.; Du, Y.; Ye, R. D.; Warshel, A. Exploring the Activation Process of the β2AR-Gs Complex. *J. Am. Chem. Soc.* **2021**, *143* (29), 11044−11051.

(9) Weis, W. I.; Kobilka, B. K. The Molecular Basis of G Protein-Coupled Receptor Activation. *Annu. Rev. Biochem.* **2018**, *87*, 897−919.

(10) Sounier, R.; Mas, C.; Steyaert, J.; Laeremans, T.; Manglik, A.; Huang, W.; Kobilka, B. K.; Déméné, H.; Granier, S. Propagation of conformational changes during μ-opioid receptor activation. *Nature* **2015**, *524* (7565), 375−378.

(11) Gregorio, G. G.; Masureel, M.; Hilger, D.; Terry, D. S.; Juette, M.; Zhao, H.; Zhou, Z.; Perez-Aguilar, J. M.; Hauge, M.; Mathiasen, S.; et al. Single-molecule analysis of ligand efficacy in β(2)AR-G-protein activation. *Nature* **2017**, *547* (7661), 68−73.

(12) Nygaard, R.; Zou, Y.; Dror, R. O.; Mildorf, T. J.; Arlow, D. H.; Manglik, A.; Pan, A. C.; Liu, C. W.; Fung, J. J.; Bokoch, M. P.; et al. The dynamic process of β(2)-adrenergic receptor activation. *Cell* **2013**, *152* (3), 532−542.

(13) Dror, R. O.; Arlow, D. H.; Maragakis, P.; Mildorf, T. J.; Pan, A. C.; Xu, H.; Borhani, D. W.; Shaw, D. E. Activation mechanism of the β2-adrenergic receptor. *Proc. Natl. Acad. Sci. U. S. A.* **2011**, *108* (46), 18684−18689.

(14) Cong, Z.; Zhao, F.; Li, Y.; Luo, G.; Mai, Y.; Chen, X.; Chen, Y.; Lin, S.; Cai, X.; Zhou, Q.; et al. Molecular features of the ligand-free GLP-1R, GCGR and GIPR in complex with Gs proteins. *Cell Discovery* **2024**, *10* (1), 18.

(15) Lin, H.; Xiao, P.; Bu, R. Q.; Guo, S.; Yang, Z.; Yuan, D.; Zhu, Z. L.; Zhang, C. X.; He, Q. T.; Zhang, C.; et al. Structures of the ADGRG2-G(s) complex in apo and ligand-bound forms. *Nat. Chem. Biol.* **2022**, *18* (11), 1196−1203.

(16) Pan, X.; Ye, F.; Ning, P.; Zhang, Z.; Li, X.; Zhang, B.; Wang, Q.; Chen, G.; Gao, W.; Qiu, C.; et al. Structural insights into ligand recognition and selectivity of the human hydroxycarboxylic acid receptor HCAR2. *Cell Discovery* **2023**, *9* (1), 118.

(17) Mafi, A.; Kim, S. K.; Goddard, W. A., 3rd. The G protein-first activation mechanism of opioid receptors by Gi protein and agonists. *QRB Discov* **2021**, *2*, No. e9.

(18) Mafi, A.; Kim, S. K.; Goddard, W. A., 3rd. The mechanism for ligand activation of the GPCR-G protein complex. *Proc. Natl. Acad. Sci. U. S. A.* **2022**, *119* (18), No. e2110085119.

(19) Huang, S. K.; Pandey, A.; Tran, D. P.; Villanueva, N. L.; Kitao, A.; Sunahara, R. K.; Sljoka, A.; Prosser, R. S. Delineating the conformational landscape of the adenosine A_{2A} receptor during G protein coupling. *Cell* **2021**, *184* (7), 1884−1894.

(20) Xu, X.; Meckel, T.; Brzostowski, J. A.; Yan, J.; Meier-Schellersheim, M.; Jin, T. Coupling Mechanism of a GPCR and a Heterotrimeric G Protein During Chemoattractant Gradient Sensing in Dictyostelium. *Science Signaling* **2010**, *3* (141), ra71−ra71.

(21) Navarro, G.; Cordomí, A.; Casadó-Anguera, V.; Moreno, E.; Cai, N.-S.; Cortés, A.; Canela, E. I.; Dessauer, C. W.; Casadó, V.; Pardo, L.; et al. Evidence for functional pre-coupled complexes of receptor heteromers and adenylyl cyclase. *Nat. Commun.* **2018**, *9* (1), 1242.

(22) Cevheroğlu, O.; Becker, J. M.; Son, Ç D. GPCR-Gα protein precoupling: Interaction between Ste2p, a yeast GPCR, and Gpa1p, its Gα protein, is formed before ligand binding via the Ste2p C-terminal domain and the Gpa1p N-terminal domain. *Biochim Biophys Acta Biomembr* **2017**, *1859* (12), 2435−2446.

(23) Ti, R.; Pang, B.; Yu, L.; Gan, B.; Ma, W.; Warshel, A.; Ren, R.; Zhu, L. Fine-tuning activation specificity of G-protein-coupled receptors via automated path searching. *Proc. Natl. Acad. Sci. U. S. A.* **2024**, *121* (8), No. e2317893121.

(24) Bolhuis, P. G.; Chandler, D.; Dellago, C.; Geissler, P. L. Transition path sampling: throwing ropes over rough mountain passes, in the dark. *Annu. Rev. Phys. Chem.* **2002**, *53*, 291−318.

(25) Maragliano, L.; Fischer, A.; Vanden-Eijnden, E.; Ciccotti, G. String method in collective variables: minimum free energy paths and isocommittor surfaces. *J. Chem. Phys.* **2006**, *125* (2), 24106.
(26) Pan, A. C.; Sezer, D.; Roux, B. Finding transition pathways using the string method with swarms of trajectories. *J. Phys. Chem. B* **2008**, *112* (11), 3432−3440.
(27) Díaz Leines, G.; Ensing, B. Path finding on high-dimensional free energy landscapes. *Phys. Rev. Lett.* **2012**, *109* (2), No. 020601.
(28) Chen, C.; Huang, Y.; Jiang, X.; Xiao, Y. A fast tomographic method for searching the minimum free energy path. *J. Chem. Phys.* **2014**, *141* (15), No. 154109.
(29) E, W.; Vanden-Eijnden, E. Transition-path theory and path-finding algorithms for the study of rare events. *Annu. Rev. Phys. Chem.* **2010**, *61*, 391−420.
(30) Moradi, M.; Enkavi, G.; Tajkhorshid, E. Atomic-level characterization of transport cycle thermodynamics in the glycerol-3-phosphate:phosphate antiporter. *Nat. Commun.* **2015**, *6*, 8393.
(31) Zhu, L.; Sheong, F. K.; Cao, S.; Liu, S.; Unarta, I. C.; Huang, X. TAPS: A traveling-salesman based automated path searching method for functional conformational changes of biological macromolecules. *J. Chem. Phys.* **2019**, *150* (12), No. 124105.
(32) Branduardi, D.; Gervasio, F. L.; Parrinello, M. From A to B in free energy space. *J. Chem. Phys.* **2007**, *126* (5), No. 054103.
(33) Xi, K.; Hu, Z.; Wu, Q.; Wei, M.; Qian, R.; Zhu, L. Assessing the Performance of Traveling-salesman based Automated Path Searching (TAPS) on Complex Biomolecular Systems. *J. Chem. Theory Comput* **2021**, *17* (8), 5301−5311.
(34) Wang, L.; Xi, K.; Zhu, L.; Da, L. T. DNA Deformation Exerted by Regulatory DNA-Binding Motifs in Human Alkyladenine DNA Glycosylase Promotes Base Flipping. *J. Chem. Inf Model* **2022**, *62* (13), 3213−3226.
(35) Wang, Y.; Dahmane, S.; Ti, R.; Mai, X.; Zhu, L.; Carlson, L.-A.; Stjepanovic, G. Structural basis for lipid transfer by the ATG2A−ATG9A complex. *Nat. Struct. Mol. Biol.* **2025**, *32*, 35.
(36) Liu, J.; Zhu, L. PlmCas12e Utilizes Glu662 to Prevent Cleavage Site Occupation by Positively Charged Residues Before Target Strand Cleavage. *Molecules* **2024**, *29* (21), 5036.
(37) Halder, R.; Chu, Z. T.; Ti, R.; Zhu, L.; Warshel, A. On the Control of Directionality of Myosin. *J. Am. Chem. Soc.* **2024**, *146* (41), 28360−28374.
(38) Xi, K.; Zhu, L. Automated Path Searching Reveals the Mechanism of Hydrolysis Enhancement by T4 Lysozyme Mutants. *International Journal of Molecular Sciences* **2022**, *23* (23), 14628.
(39) Latorraca, N. R.; Venkatakrishnan, A. J.; Dror, R. O. GPCR Dynamics: Structures in Motion. *Chem. Rev.* **2017**, *117* (1), 139−155.
(40) Nagasawa, T.; Hirota, S.; Tachibana, K.; Takakura, N.; Nishikawa, S.; Kitamura, Y.; Yoshida, N.; Kikutani, H.; Kishimoto, T. Defects of B-cell lymphopoiesis and bone-marrow myelopoiesis in mice lacking the CXC chemokine PBSF/SDF-1. *Nature* **1996**, *382* (6592), 635−638.
(41) McGrath, K. E.; Koniski, A. D.; Maltby, K. M.; McGann, J. K.; Palis, J. Embryonic expression and function of the chemokine SDF-1 and its receptor, CXCR4. *Dev. Biol.* **1999**, *213* (2), 442−456.
(42) Möhle, R.; Bautz, F.; Rafii, S.; Moore, M. A. S.; Brugger, W.; Kanz, L. The chemokine receptor CXCR-4 is expressed on CD34+ hematopoietic progenitors and leukemic cells and mediates transendothelial migration induced by stromal cell-derived factor-1. *Blood* **1998**, *91* (12), 4523−4530.
(43) Dar, A.; Kollet, O.; Lapidot, T. Mutual, reciprocal SDF-1/CXCR4 interactions between hematopoietic and bone marrow stromal cells regulate human stem cell migration and development in NOD/SCID chimeric mice. *Exp Hematol* **2006**, *34* (8), 967−975.
(44) Jo, S.; Kim, T.; Iyer, V. G.; Im, W. CHARMM-GUI: a web-based graphical user interface for CHARMM. *J. Comput. Chem.* **2008**, *29* (11), 1859−1865.
(45) Dewan, M. Z.; Ahmed, S.; Iwasaki, Y.; Ohba, K.; Toi, M.; Yamamoto, N. Stromal cell-derived factor-1 and CXCR4 receptor interaction in tumor growth and metastasis of breast cancer. *Biomed Pharmacother* **2006**, *60* (6), 273−276.
(46) Huang, C. Y.; Lee, C. Y.; Chen, M. Y.; Yang, W. H.; Chen, Y. H.; Chang, C. H.; Hsu, H. C.; Fong, Y. C.; Tang, C. H. Stromal cell-derived factor-1/CXCR4 enhanced motility of human osteosarcoma cells involves MEK1/2, ERK and NF-kappaB-dependent pathways. *J. Cell Physiol* **2009**, *221* (1), 204−212.
(47) Liao, Y. X.; Zhou, C. H.; Zeng, H.; Zuo, D. Q.; Wang, Z. Y.; Yin, F.; Hua, Y. Q.; Cai, Z. D. The role of the CXCL12-CXCR4/CXCR7 axis in the progression and metastasis of bone sarcomas (Review). *Int. J. Mol. Med.* **2013**, *32* (6), 1239−1246.
(48) Jørgensen, A. S.; Daugvilaite, V.; De Filippo, K.; Berg, C.; Mavri, M.; Benned-Jensen, T.; Juzenaite, G.; Hjortø, G.; Rankin, S.; Våbenø, J.; et al. Biased action of the CXCR4-targeting drug plerixafor is essential for its superior hematopoietic stem cell mobilization. *Commun. Biol.* **2021**, *4* (1), 569.
(49) Bleul, C. C.; Wu, L.; Hoxie, J. A.; Springer, T. A.; Mackay, C. R. The HIV coreceptors CXCR4 and CCR5 are differentially expressed and regulated on human T lymphocytes. *Proc. Natl. Acad. Sci. U. S. A.* **1997**, *94* (5), 1925−1930.
(50) Chatterjee, S.; Behnam Azad, B.; Nimmagadda, S. The intricate role of CXCR4 in cancer. *Adv. Cancer Res.* **2014**, *124*, 31−82.
(51) Döring, Y.; Pawig, L.; Weber, C.; Noels, H. The CXCL12/CXCR4 chemokine ligand/receptor axis in cardiovascular disease. *Front. Physiol.* **2014**, *5*, 212.
(52) Domanska, U. M.; Kruizinga, R. C.; Nagengast, W. B.; Timmer-Bosscha, H.; Huls, G.; de Vries, E. G.; Walenkamp, A. M. A review on CXCR4/CXCL12 axis in oncology: no place to hide. *Eur. J. Cancer* **2013**, *49* (1), 219−230.
(53) Tchernychev, B.; Ren, Y.; Sachdev, P.; Janz, J. M.; Haggis, L.; O'Shea, A.; McBride, E.; Looby, R.; Deng, Q.; McMurry, T.; et al. Discovery of a CXCR4 agonist pepducin that mobilizes bone marrow hematopoietic cells. *Proc. Natl. Acad. Sci. U. S. A.* **2010**, *107* (51), 22255−22259.
(54) Negro, S.; Zanetti, G.; Mattarei, A.; Valentini, A.; Megighian, A.; Tombesi, G.; Zugno, A.; Dianin, V.; Pirazzini, M.; Fillo, S.; et al. An Agonist of the CXCR4 Receptor Strongly Promotes Regeneration of Degenerated Motor Axon Terminals. *Cells* **2019**, *8* (10), 1183.
(55) Li, K.; Chuen, C. K.; Lee, S. M.; Law, P.; Fok, T. F.; Ng, P. C.; Li, C. K.; Wong, D.; Merzouk, A.; Salari, H.; et al. Small peptide analogue of SDF-1alpha supports survival of cord blood CD34+ cells in synergy with other cytokines and enhances their ex vivo expansion and engraftment into nonobese diabetic/severe combined immunodeficient mice. *Stem Cells* **2006**, *24* (1), 55−64.
(56) Qin, L.; Kufareva, I.; Holden, L. G.; Wang, C.; Zheng, Y.; Zhao, C.; Fenalti, G.; Wu, H.; Han, G. W.; Cherezov, V.; et al. Structural biology. Crystal structure of the chemokine receptor CXCR4 in complex with a viral chemokine. *Science* **2015**, *347* (6226), 1117−1122.
(57) Wu, B.; Chien, E. Y.; Mol, C. D.; Fenalti, G.; Liu, W.; Katritch, V.; Abagyan, R.; Brooun, A.; Wells, P.; Bi, F. C.; et al. Structures of the CXCR4 chemokine GPCR with small-molecule and cyclic peptide antagonists. *Science* **2010**, *330* (6007), 1066−1071.
(58) Liu, Y.; Liu, A.; Li, X.; Liao, Q.; Zhang, W.; Zhu, L.; Ye, R. D. Cryo-EM structure of monomeric CXCL12-bound CXCR4 in the active state. *Cell Rep* **2024**, *43* (8), No. 114578.
(59) Zhou, Q.; Yang, D.; Wu, M.; Guo, Y.; Guo, W.; Zhong, L.; Cai, X.; Dai, A.; Jang, W.; Shakhnovich, E. I.; et al. Common activation mechanism of class A GPCRs. *Elife* **2019**, *8*, No. e50279.
(60) Kooistra, A. J.; Mordalski, S.; Pándy-Szekeres, G.; Esguerra, M.; Mamyrbekov, A.; Munk, C.; Keserű, G. M.; Gloriam, D. E. GPCRdb in 2021: integrating GPCR sequence, structure and function. *Nucleic Acids Res.* **2021**, *49* (D1), D335−d343.
(61) Schlitter, J.; Engels, M.; Krüger, P. Targeted molecular dynamics: a new approach for searching pathways of conformational transitions. *J. Mol. Graph* **1994**, *12* (2), 84−89.
(62) Kästner, J. Umbrella sampling. *Wiley Interdiscip. Rev.: Comput. Mol. Sci.* **2011**, *1* (6), 932−942.
(63) Stephens, B. S.; Ngo, T.; Kufareva, I.; Handel, T. M. Functional anatomy of the full-length CXCR4-CXCL12 complex systematically

dissected by quantitative model-guided mutagenesis. *Sci. Signaling* **2020**, *13* (640), No. eaay5024.
(64) Powers, A. S.; Pham, V.; Burger, W. A. C.; Thompson, G.; Laloudakis, Y.; Barnes, N. W.; Sexton, P. M.; Paul, S. M.; Christopoulos, A.; Thal, D. M.; et al. Structural basis of efficacy-driven ligand selectivity at GPCRs. *Nat. Chem. Biol.* **2023**, *19* (7), 805−814.
(65) Wu, Y.; Li, X.; Hua, T.; Liu, Z. J.; Liu, H.; Zhao, S. MD Simulations Revealing Special Activation Mechanism of Cannabinoid Receptor 1. *Front Mol. Biosci* **2022**, *9*, No. 860035.
(66) Blanchet, X.; Langer, M.; Weber, C.; Koenen, R. R.; von Hundelshausen, P. Touch of chemokines. *Front Immunol* **2012**, *3*, 175.
(67) Flock, T.; Ravarani, C. N. J.; Sun, D.; Venkatakrishnan, A. J.; Kayikci, M.; Tate, C. G.; Veprintsev, D. B.; Babu, M. M. Universal allosteric mechanism for Gα activation by GPCRs. *Nature* **2015**, *524* (7564), 173−179.
(68) Bumbak, F.; Pons, M.; Inoue, A.; Paniagua, J. C.; Yan, F.; Wu, H.; Robson, S. A.; Bathgate, R. A. D.; Scott, D. J.; Gooley, P. R.; et al. Ligands selectively tune the local and global motions of neurotensin receptor 1 (NTS1). *Cell Rep.* **2023**, *42* (1), No. 112015.
(69) Huang, S. K.; Prosser, R. S. Dynamics and mechanistic underpinnings to pharmacology of class A GPCRs: an NMR perspective. *American Journal of Physiology-Cell Physiology* **2022**, *322* (4), C739−C753.
(70) Frere, G.; Pandey, A.; Gould, J.; Hasabnis, A.; Gunning, P. T.; Prosser, R. S. The Application of F NMR to Studies of Protein Function and Drug Screening. In *GPCRs as Therapeutic Targets*; Wiley: 2022; pp 874−896.
(71) Mafi, A.; Kim, S. K.; Goddard, W. A., 3rd. The dynamics of agonist-β(2)-adrenergic receptor activation induced by binding of GDP-bound Gs protein. *Nat. Chem.* **2023**, *15* (8), 1127−1137.
(72) Jaracz-Ros, A.; Bernadat, G.; Cutolo, P.; Gallego, C.; Gustavsson, M.; Cecon, E.; Baleux, F.; Kufareva, I.; Handel, T. M.; Bachelerie, F.; et al. Differential activity and selectivity of N-terminal modified CXCL12 chemokines at the CXCR4 and ACKR3 receptors. *J. Leukoc Biol.* **2020**, *107* (6), 1123−1135.
(73) Quoyer, J.; Janz, J. M.; Luo, J.; Ren, Y.; Armando, S.; Lukashova, V.; Benovic, J. L.; Carlson, K. E.; Hunt, S. W., 3rd; Bouvier, M. Pepducin targeting the C-X-C chemokine receptor type 4 acts as a biased agonist favoring activation of the inhibitory G protein. *Proc. Natl. Acad. Sci. U. S. A.* **2013**, *110* (52), E5088−5097.

https://doi.org/10.1021/jacs.4c14293
J. Am. Chem. Soc. 2025, 147, 10129−10138